Numerical Simulations of Smoke Movement and Coagulation

YUKIO YAMAUCHI
R & D Center, Hochiki Corp.
246 Tsuruma, Machida-shi, Tokyo 194, Japan

ABSTRACT

For the purpose of understanding the smoke detector's response to enclosure fires, a computational model for predicting the evolution of the local concentration and size distribution of smoke aerosol is presented. The model utilizes the characteristic of smoke aerosol that the large size part of the size distribution is not significantly affected by coagulation and that its size distribution takes a virtually time-independent reduced form. By numerically solving the conservation equations of total particle volume and total particle number, the size distribution of the smoke aerosol is determined by the reduced expression of the size distribution where the total particle volume and the total particle number are the parameters. The results of sample calculations and relevant experiments showed a reasonable agreement.

Key words: Aerosols; enclosure fires; detector sensitivity; fire detectors; modeling; particle size; room fires; simulation; smoke detectors.

INTRODUCTION

Smoke detectors are an effective means for early detection of fires in enclosures. Light scattering type smoke detectors and ionization type smoke detectors are mostly in use. However, the response of these detectors is strongly dependent on the particle size of the smoke aerosol and its concentration [1,2,3]. Since the particle size distribution and the concentration of smoke aerosol vary during the evolution of the fire, fire tests have been the only tools for evaluating the detector response [4].

The variation in the size distribution of smoke aerosol is explained as a result of the phenomenon of particle coagulation due to the Brownian collisions [5]. In order to predict the detector response to a given fire in an enclosure it is necessary to evaluate the effect of coagulation as well as the large scale smoke movement.

The purpose of this report is to present a computational procedure for predicting the evolution of the local concentration and size distribution of smoke aerosol in an enclosure containing a fire source. The procedure utilizes the findings of Mulholland, et al. [6] that the large size part of the size distribution of smoke aerosol is not greatly affected by coagulation and that its size distribution takes a virtually time-independent reduced form:

$$\zeta = 0.1\ (\eta + 0.1)^{-2}, \qquad (1)$$

where ζ and η are the reduced number distribution and the reduced particle volume respectively. The corresponding unreduced size distribution is

$$n(v,t) = 0.1V[v + 0.1V/N(t)]^{-2}. \quad (2)$$

This suggests that if the total particle volume V and the total particle number N are given the number distribution n as a function of particle volume v is determined by Eq. (2).

In this paper a computational model for predicting the total particle volume V and the total particle number N locally and thus predicting the local size distribution and concentration of smoke aerosol is described. In order to validate the theoretical model the predictions were compared with some experimental data.

THEORETICAL MODEL

Smoke Movement

Smoke aerosol generated at the heat/smoke source is transported by the velocity field of buoyant convection. Thermal molecular diffusion also plays a small role. Regarding the smoke concentration (mass, volume or number) as a passively-transported scalar quantity in the field, its time averaged conservation equation for the constant density flows takes the form:

$$\frac{\delta C}{\delta t} + \frac{\delta Cu_j}{\delta x_j} = \frac{\delta}{\delta x_j}\left(D^* \frac{\delta C}{\delta x_j}\right) + S, \quad (3)$$

where C is the smoke concentration; u_i $(i,j = 1,2,3)$ is the component velocity in the direction x_i; D^* is the effective diffusion coefficient; S is the source/sink term. The effective diffusion coefficient D^* is the combined laminar and turbulent diffusions defined by

$$D^* = D + K \quad (4)$$

where D and K respectively are the laminar and turbulent diffusion coefficient.

Assuming that the wall adsorption and settling of aersol are insignificant, the source/sink term in the conservation equation of total particle volume can be neglected except at the point of heat/smoke source:

$$\frac{\delta V}{\delta t} + \frac{\delta Vu_j}{\delta x_j} = \frac{\delta}{\delta x_j}\left(D^* \frac{\delta V}{\delta x_j}\right) \quad (5)$$

where $V = V(x_i,t)$ is the total particle volume of smoke aerosol within a unit volume at the point x_i at at the time t.

Smoke Coagulation

Smoke particles moving in the enclosure collide and adhere with each other as a result of the Brownian motion. Through this process the average particle size increases while the total number of particles decreases. The coagulation frequency is closely related to the temperature and the size of the aerosol particles and its concentration.

The basic equation for the variation of the number of aerosol particles versus time due to thermal coagulation takes the form:

$$\left[\frac{\delta\, n(x_i,v,t)}{\delta\, t}\right]_{int} = \int_0^v \Gamma(v-v',v')\; n(x_i,v-v',t)\; n(x_i,v',t)\; dv$$

$$- 2\; n(x_i,v,t) \int_0^\infty \Gamma(v,v')\; n(x_i,v',t)\; dv' \qquad (6)$$

where $n(x_i,v,t)dv$ means the number of aerosol particles at the point x_i at the time t, whose volume lies between the values of v and v + dv; $\Gamma(v,v')$ is the coagulation coefficient between aerosol particles of volumes of v and v'. Subscript 'int' denotes that only the internal process within the idealized spatial volume element is concerned here.

Eq. (6) is so complicated that an analytical solution is very difficult to find. Trying to get numerical solution of the equation is impractical because of the wide range of particle size (roughly 0.01 to 10 μm in diameter) concerned.

Assuming that the coagulation coefficient (Γ) is not affected by the flow fields and assuming Γ is independent of particle size, then we find by integrating over particle volume:

$$\left[\frac{\delta N}{\delta t}\right]_{int} = -\Gamma_0 N^2 \qquad (7)$$

where $N = N(x_i,t)$ is the total number of particles within a unit volume at the point x_i at the time t. As the size distribution can be estimated using Eq. (2), this assumption is quite useful.

Building this relation into the source/sink term of Eq. (3) we get a conservation equation for the total particle number:

$$\frac{\delta N}{\delta t} + \frac{\delta N u_j}{\delta x_j} = \frac{\delta}{\delta x_j}\left(D^* \frac{\delta N}{\delta x_j}\right) - \Gamma_0 N^2. \qquad (8)$$

Given the velocity field as a function of time Eqs. (5) and (8) can be solved numerically by giving the generation term as part of the boundary conditions.

Natural Convection

Our next problem is the prediction of flow fields in the enclosure. For our sample calculations, which were two-dimensional, the following set of time-averaged equations for constant density flows were used. The equation of vorticity transport was derived from the Navier-Stokes' type equation of motion by eliminating the pressure term. In representing the influence of buoyancy, the Boussinesq approximation is incorporated. The buoyancy term is included in the equation of vorticity transport as $g\beta\, \delta\theta / \delta x$.

Equation of energy

$$\frac{\delta \theta}{\delta t} + u_x \frac{\delta \theta}{\delta x} + u_y \frac{\delta \theta}{\delta y} = \alpha^* \left(\frac{\delta^2 \theta}{\delta x^2} + \frac{\delta^2 \theta}{\delta y^2}\right) \qquad (9)$$

Equation of stream function

$$u_x = \frac{\delta \psi}{\delta y}, \qquad u_y = -\frac{\delta \psi}{\delta x}, \tag{10}$$

Equation of scalar vorticity

$$\omega = \frac{\delta u_y}{\delta x} - \frac{\delta u_x}{\delta y} = -\left(\frac{\delta^2 \psi}{\delta x^2} + \frac{\delta^2 \psi}{\delta y^2}\right), \tag{11}$$

Equation of vorticity transport

$$\frac{\delta \omega}{\delta y} + u_x \frac{\delta \omega}{\delta x} + u_y \frac{\delta \omega}{\delta y} = \nu^* \left(\frac{\delta^2 \omega}{\delta x^2} + \frac{\delta^2 \omega}{\delta y^2}\right) + g\beta \frac{\delta \theta}{\delta x}. \tag{12}$$

Here θ is the temperature; ψ is the stream function; ω is the scalar vorticity; α^* is the effective heat diffusivity; ν^* is the effective kinematic viscosity; g is the gravitational acceleration; β is the volumetric expansion coefficient.

COMPUTATIONAL AND EXPERIMENTAL PROCEDURE

In order to validate the theoretical model, we experimented using a rectangular enclosure. Numerical simulations were applied to the two-dimensional enclosure having the same dimensions. Both results were compared.

Smoke Source Evaluation

Cotton wicks were used for both the heat and smoke source. This material is used by Underwriters' Laboratories, Inc. (UL) for testing smoke detectors in Standard No. 268. Prior to the enclosure experiments and calculations, the size distribution and the generation rates of smoke aerosol were evaluated using a smoke box of the size 1.6 x 0.8 x 0.5 m.

Three cotton wicks were set glowing then held inside the smoke box for 60 seconds. After allowing the smoke to become well mixed (1 min) by a fan positioned inside the box, the size distribution was measured as a function of time using an optical particle counter (Particle Measuring Systems, Inc. model LAS-X). In order to keep the concentration of aerosol within the measuring range, a 100 to 1 or 200 to 1 diluter was used in the sampling line of the optical particle counter. It took about 40 seconds for measuring the size range of 0.09 - 3.0 μm. Light extinction by the smoke aerosol inside the box was monitored using an extinction meter equivalent to UL 268 specifications.

The measured size distribution of cotton wick smoke is plotted in Fig. 1, where the readings of the optical particle counter is converted into values of size disribution, dn/dv, by assuming the particle shape as spherical. The observed light extinction coefficient for this size distribution was about 2.5 %/m. The effect of coagulation was insignificant in this level of aerosol concentration.

The measured particle size distribution showed a good agreement with the estimated size distribution by Eq. (2). Reversely by assuming that the size distribution follows Eq. (2) even outside the measured range, the generation rates of smoke aerosol in total number N and total volume V were calculated. The calculated aersol generation rates of a single glowing cotton wick are

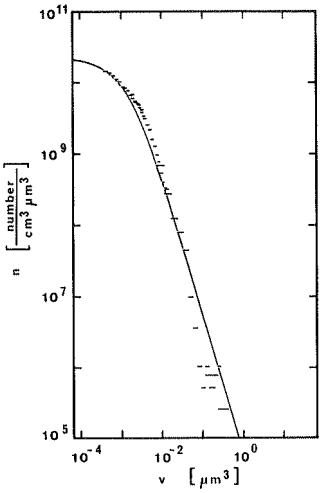

FIGURE 1. The measured size distribution of smoke aerosol from glowing cotton wicks. The dashes (-) show the data points. The solid line shows the assumed size distribution used for the calculations.

$dN/dt = 1.2 \times 10^{11}$ particles/sec and $dV/dt = 1.9 \times 10^{9}\ \mu m^3/sec$. These values give the average particle volume of $\bar{v} = 1.6 \times 10^{-2}\ \mu m^3$.

Experimental Setup

The size of the enclosure is 1.8 m W. x 1.6 m H. x 0.9 m D. with a hung wall of 0.4 m down at the open end (Fig. 2). The interior surface of the enclosure was made of polystyrene foam thermal insulator. 20 glowing cotton wicks were positioned in line embedded at the center of the floor. The scalar velocity was measured at three different places in order to check the flow reproducibility. A thermal anemometer (Nihon Kagaku Kogyo Co. Ltd. model 6181) was used for measuring the velocity. The same optical particle counter and diluter described above were used for measuring the aerosol size distribution.

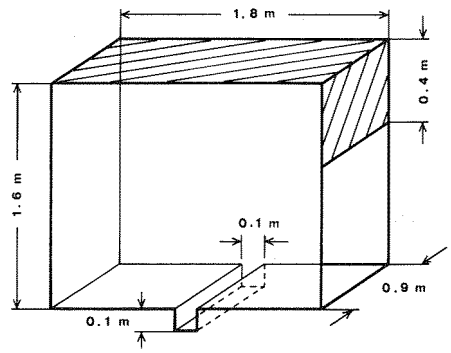

FIGURE 2. The experimental enclosure.

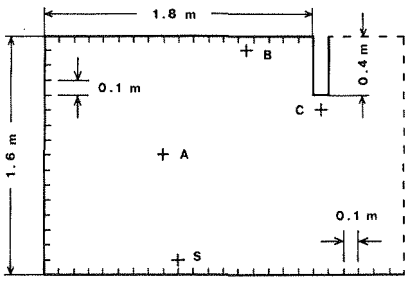

FIGURE 3. The computational domain: S shows the heat/smoke source. A, B and C show the points where comparison with the experiments was made.

The flow state in the enclosure became steady in about 3 min after beginning the experiment. The data taken at 4 min (240 sec) were used for the comparison.

Numerical Calculations

Fig. 3 shows the computational domain of the simulation. For computational purposes the domain was extended to the free boundary region outside the doorway. The letter S shows the point of heat/smoke source. A, B and C show the points where comparison with the experiments was made.

Computational scheme. The finite difference method was used for the numerical calculations. In deriving the finite difference equations the two-point backward implicit scheme was employed for all the time derivatives. For the spatial derivatives, the up-wind difference and central difference schemes were taken for the convective and non-convective terms respectively.

Boundary and initial conditions. The two types of boundary, solid or free, have to be considered. On the solid boundaries the non-slip condition was employed on the velocity components, thus the stream function on the interior walls was set to be constant. For the temperature equation, adiabatic side walls and adiabatic ceiling were used. The temperature of the floor was kept constant (ambient) except at the nearest point to the heat/smoke source where adiabatic conditions were taken. For the smoke concentration equations, adiabatic conditions were used for all the interior walls. The vorticity on the solid boundary was calculated by assuming the mirror points in the stream function. On the free boundaries, the derivatives of stream function and vorticity normal to the free surfaces were equated to zero. The temperature and the smoke concentration conditions were separated by the flow directions. At points of in-flow, ambient temperature and zero concentration were specified, at points of out-flow the derivatives of each variable normal to the surface were equated to zero.

As the intial conditions, the fluid in the enclosure was set motionless, uniform ambient temperature (293 K) and zero smoke concentration.

Computational details. A 17 x 26 grid system was used for the calculations. The computational time step was set as 0.1 sec. The physical constants used were as follows: the effective heat diffusivity $\alpha^* = 6.0 \times 10^{-3}$ m^2/sec, the effective kinematic viscosity $\nu^* = 6.0 \times 10^{-3}$ m^2/sec, the effective diffusion coefficient $D^* = 6.0 \times 10^{-3}$ m^2/sec, the coagulation coefficient $\Gamma_o = 4.0 \times 10^{-10}$ cm^3/sec, the volumetric expansion coefficient $\beta = 1/273$ deg^{-1}, and the gravitational acceleration g = 9.8 m/sec^2.

α^*. ν^* and D^* were set to be contant and have the same value of 400ν. For the value of Γ_0, the coagulation coefficient, the suggested value for the punk smoke by Lee and Mulholland [5] was used.

Constant heat and smoke generation were assumed and simulated by injecting additional quantities at each time step into the idealized mesh cell at the heat/smoke source. The experimentally determined values described in the previous section were used for the smoke generation. The temperature rise rate of 10 deg/sec was assumed from observations and used for the heat generation.

It took about 30 min computational run time for the calculation up t = 240 sec using IBM 370 computer system.

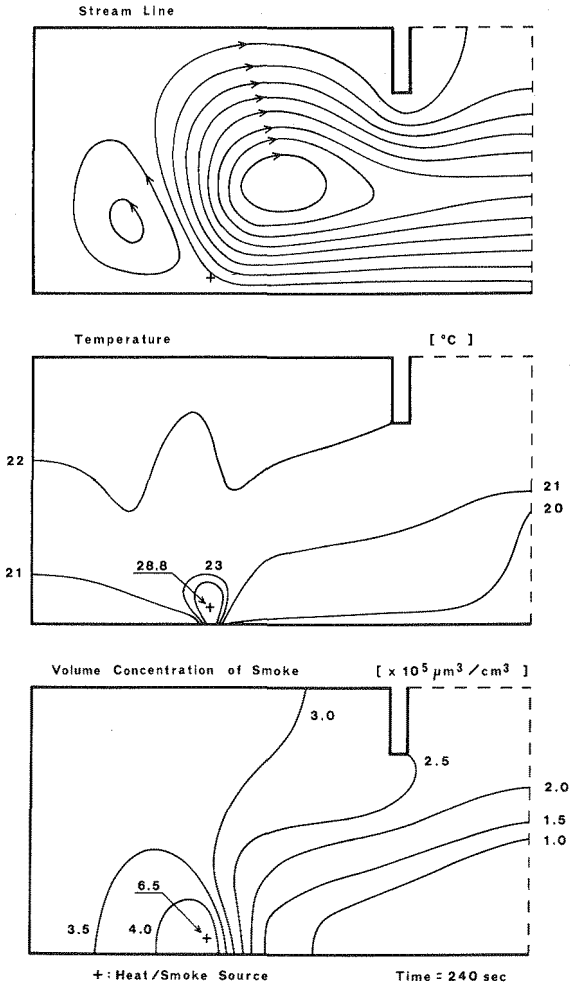

FIGURE 4. Contours of calculated stream function, temperature and smoke concentration.

TABLE 1. The observed and calculated quantities of scalar velocity.

	Point A	Point B	Point C
Observed velocity (cm / sec)	8.0	4.0	6.0
Calculated velocity (cm / sec)	7.2	1.8	3.6

RESULTS AND DISCUSSIONS

Contours of calculated stream function, temperature and smoke concentration at the time of 240 sec are shown in Fig. 4. All the values represent the spatially averaged values in each idealized mesh cell (10 x 10 cm). The difference between the contour plots for the temperature and for the smoke concentration - both are the passively-transported physical quantities - came from the difference of boundary conditions on the floor. Adiabatic conditions were taken for the smoke concentration while the temperature of the floor was fixed to be ambient (293 K) since almost no temperature rise was observed in the experiments.

The reproducibility of the calculation of flow pattern was checked by comparing with the observed quantities of scalar velocity. The observed and calculated quantities at three different places (A, B, C) are tabulated in Tab. 1. These points were selected as to represent respectively the plume flow, the ceiling flow and the out-flow from the enclosure. The quantity of the velocity in the plume region was reproduced well, while the quantities of the velocity at the points adjacent to the ceiling and to the under edge of the hung wall were under-estimated by the factor of about 1/2. Since the effective kinematic viscosity ν^* was assumed to be constant, more precise agreement would not be expected.

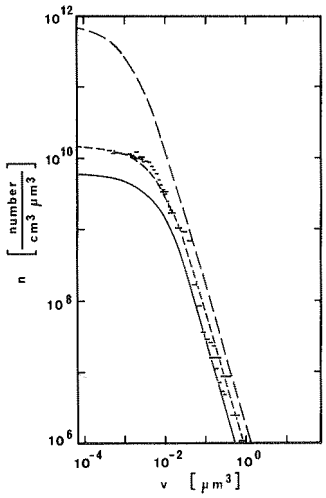

FIGURE 5. The measured and calculated size distribution at point C at the time 240 sec. The solid line shows the calculated size distribution using the experimental data. The short-dashed line show the calculated result using the modified generation rates and coagulation coefficient. For comparison the size distribution at the heat/smoke source is plotted by long dashes.

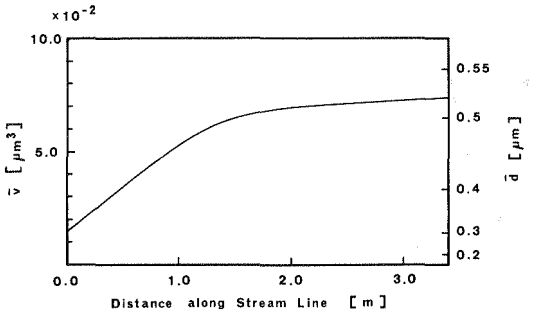

FIGURE 6. The variation of the calculated average particle volume $\bar{v}$ versus travel distance along the stream line from the heat/smoke source.

Fig. 5 shows the measured and calculated size distribution of smoke aerosol at point C at the time 240 sec. Although the calculated size distribution using the experimentally determined aerosol generation rates gave a good reproduction in the profile of the size distribution, the volume concentration was 2.7 times under-estimated compared with the experimental data. Calculations with modified generation rates and modified coagulation coefficients were made and one of the results is also plotted in Fig. 5. The data set used in this case were $dV/dt = 3.24 \times 10^{11}$ particles/sec, $dN/dt = 5.13 \times 10^{9}\ \mu m^3$/sec and $\Gamma_0 = 1.5 \times 10^{-10}$ cm^3/sec.

Fig. 6 shows the variation of the calculated average particle volume $\bar{v}$ versus travel distance along the stream line from the heat/smoke source. This result suggests that the coagulation of aerosol occurs mostly in the plume region and becomes insignificant in the ceiling flow.

The reason why we had to adjust the values of the smoke generation rates and the coagulation coefficient have to be discussed here. Not only these parameters but also the diffusion coefficient (D^*) have the effect of varying the coagulation frequency. Smaller D^* increases the smoke concentration in the plume region and in effect increases the average particle volume ($\bar{v}$) at the ceiling. Thus only the realistic values of the smoke generation rates, the coagulation coefficient and the diffusion coefficient should give a good reproduction of the phenomena. Since the exact values for these parameters were unknown, the values of the smoke generation rates and the coagulation coefficient were adjusted. As far as the detector response is concerned, this adjustment would not reduce the utility of this model. Baum et al. reported a somewhat similar study of simulating the fire induced flow and smoke coagulation [7]. In their model the smoke movement was simulated by the particle tracking method which corresponds to D^* equal zero in Eqs. (5) and (8). We conducted calculations with $D^* = 0$, which gave larger average particle volume at the ceiling.

It has become clear that a deterministic approach to understand the detector's response to enclosed fire is possible. This will allow us to utilize the computational model as a development tool in the software for signal processing of 'intelligent' fire detection systems such as described in [8,9].

ACKNOWLEDGEMENTS

The author is grateful to Professor Takashi Handa of Science University of Tokyo for continuous advice and encouragement. The author also wish to thank Dr. Masahiro Morita of Science University of Tokyo for his invaluable advice on the computational schemes.

NOMENCLATURE

C,	smoke concentration;
D,	diffusion coefficient (laminar);
D^*,	effective diffusion coefficient;
g,	gravitational acceleration;
K,	turbulent diffusion coefficient;
N,	total particle number;
n,	particle number distribution;
S,	source or sink for the smoke concentration;
t,	time;
u_i,	velocity component in x_i axis (i = 1,2,3);
V,	total particle volume;
v,	particle volume;
$\bar{v}$	average particle volume;
x_i,	cartesian coordinates (i = 1,2,3);
x, y,	horizontal and vertical coordinates;

Greek letters

α^*,	effective heat diffusivity;
β,	volumetric expansion coefficient;
Γ,	coagulation coefficient;
ζ,	reduced number distribution;
η,	reduced particle volume;
θ,	absolute temperature;
ν^*,	effective kinematic viscosity;
ψ,	stream function;
ω,	scalar vorticity.

REFERENCES

1. Welker, R. W. and Wagner, J. P.: "Particle Size and Mass Distributions of Selected Smokes. Effect on Ionization Detector Response," J. fire & Flamability, 8: 26 - 37, 1977.

2. Bukowski, R. W. and Mulholland, G. W.: "Smoke Detector Design and Smoke Properties," Nat. Bur. Stand. (U.S.), Tech. Note 973, 1978.

3. Mulholland, G. W. and Liu, B. Y. H.: "Response of Smoke Detectors to Monodisperse Aerosols," J. Research Nat. Bur. Stand., 85: 3, 223 - 238, 1980.

4. Bukowski, R. W. and Bright, R. G.: "Results of Full-Scale Fire Tests with Photoelectric Smoke Detectors," Nat. Bur. Stand. (U.S.), NBSIR 75-700, 1975.

5. Lee. T. G. K., and Mulholland. G. W.: "Physical Properties of Smokes Pertinent to Smoke Detector Technology," Nat. Bur. Stand. (U.S.), NBSIR 77-1312, 1977.

6. Mulholland, G. W., Lee, T. G. and Baum, H. R.: "The Coagulation of Aerosols with Broad Initial Size Distributions," J. Collid and Interface Science, 62: 3, 406 - 420, 1977.

7. Baum H. R., Rehm R. G. and Mulholland G. W.: "Computation of Fire Induced Flow and Smoke Coagulation," 19th Symposium (International) on Combustion/The Combustion Inst., 921 - 931, 1982.

8. Scheidweiler, A.: "The Distribution of Intelligence in Future Fire Detection Systems," Fire Safety J., 6: 3, 209 - 214, 1983.

9. Tomkewitsch, R.: "Fire Detector Systems with 'Distributed Intelligence'- The Pulse Polling System," Fire Safety J., 6: 3, 225 - 232, 1983.